



# Synthesis, characterization and electrochemical investigation of hetaryl chromium(0) aminocarbene complexes

Radka Metelková<sup>a,b</sup>, Tomáš Tobrman<sup>a</sup>, Hana Kvapilová<sup>a,b</sup>, Irena Hoskovcová<sup>a,1</sup>, Jiří Ludvík<sup>b,\*</sup>

<sup>a</sup> Prague Institute of Chemical Technology, Technická 5, 166 28 Prague 6, Czech Republic

<sup>b</sup> J. Heyrovský Institute of Physical Chemistry, Academy of Science of the Czech Republic, Dolejškova 3, 182 23 Prague 8, Czech Republic

## ARTICLE INFO

### Article history:

Received 29 February 2012

Received in revised form 30 April 2012

Accepted 1 May 2012

Available online 14 May 2012

### Key words:

Fischer aminocarbene complexes

Synthesis

Electrochemical oxidation and reduction

Structure–reactivity relationship

DFT

## ABSTRACT

Fischer carbene complexes are useful precursors in organic synthesis and promising catalysts. For both these purposes, a fine “tuning” of their thermodynamic properties and reactivity is of high interest. Therefore a detailed insight into the structure–reactivity correlation is necessary for aimed design and synthesis of compounds with required specific properties.

In this contribution a new series of aminocarbene complexes of chromium(0) was synthesized, where the originally used phenyl substituent in the compound **I** pentacarbonyl[(*N,N*-dimethylamino)(phenyl)carbene]chromium(0), was replaced by various five-membered heteroaromatic rings: furan (**II**), thiophene (**III**) and *N*-Me-pyrrol (**IV**), attached either by their position 2 or 3 (Fig. 1). The compounds were characterized by <sup>1</sup>H and <sup>13</sup>C NMR and elemental analysis. In the second part of this work an electrochemical investigation in acetonitrile followed in order to understand more deeply the oxidation and reduction process and to analyze the relative contribution of inductive and mesomeric effects of the heterocycles to the reduction of the chromium aminocarbenes. Their electrochemical behavior was compared with that obtained for the phenyl derivative **I**, the interpretation was correlated with quantum chemical calculations and the differences were discussed.

© 2012 Elsevier Ltd. All rights reserved.

## 1. Introduction

Carbene complexes are characterized by presence of a formally double bond M=CR<sub>2</sub> between the central metal atom M and the carbene ligand, =CR<sub>2</sub>. Commonly, these compounds are divided into three groups with respect to the nature of the metal–carbon bond: Electrophilic Fischer carbenes, nucleophilic Schrock carbenes and *N*-heterocyclic carbenes.

Studied chromium aminocarbene complexes belong to the Fischer type. The molecule is composed of a central metal in a low oxidation state, π-electron acceptor ligands (CO) and π-donor substituents on the methylene group (alkoxy or amino), resulting in M<sup>δ−</sup>=C<sup>δ+</sup> polarity of the metal–carbene carbon bond.

Fischer carbene complexes are useful precursors in organic synthesis [1–3] and promising catalysts [4,5]. For both these purposes, a fine modification of their reactivity is of high interest, so a detailed insight into the structure–reactivity relationship facilitates future aimed syntheses of compounds with required specific properties.

In our previous studies, we have investigated oxidation and reduction of about 40 aminocarbene complexes of general formula (CO)<sub>n</sub>M=C(NR'<sub>2</sub>)R, where R stands for *p*-substituted benzene ring, M is either chromium or tungsten (*n*=5), or M means iron (*n*=4). *E*<sub>ox</sub> and *E*<sub>red</sub> values of an extensive series of various derivatives were treated using linear free energy relationship (LFER) approach [6] to analyze the influence of structural modifications on redox properties [7,8].

The aminocarbene complexes represent molecules with two redox active centers where the oxidation process takes part at the metal atom and the reduction proceeds on the carbene “non-innocent” ligand [9,10]. As a result, the oxidation potential can be influenced by the metal itself and by the number of CO-ligands; the reduction potential can be tuned by a change of the structure and substitution of the carbene moiety.

It was recently found [11] that in the case of the mentioned aminocarbenes, the attached phenyl ring with its substituents plays a significant role in the shape and distribution of the LUMO orbital, in other words, in the extent of electron delocalization. This quality is then strongly reflected in the reduction potential.

In this contribution a new series of aminocarbene complexes of chromium(0) was synthesized, where the originally used phenyl was replaced by various five-membered heteroaromatic rings: furan (**II**), thiophene (**III**) and *N*-Me-pyrrol (**IV**), attached either by their position 2 or 3 (Fig. 1). The compounds were characterized

\* Corresponding author. Tel.: +420 266 053 217; fax: +420 286 582 307.

E-mail addresses: irena.hoskovcova@vscht.cz (I. Hoskovcová),

jiri.ludvik@jh-inst.cas.cz (J. Ludvík).

<sup>1</sup> ISE member.



## 2.2. DFT calculations

Ground state electronic structure calculations have been done by density-functional theory (DFT) method using Gaussian 09 [13] program package. B3LYP hybrid functional [14,15] was used together with 6-311g(d) polarized triple- $\zeta$  basis sets [16,17] for H, C, N, O, S and Cr atoms.

Geometry of all the complexes was optimized without any symmetry constrains, vibrational analysis was used for characterization of stationary points. For proper minima no imaginary frequencies were found. MO analysis was done at optimized structures using the same level of theory. MO plots were generated by the GaussView software.

## 2.3. Synthesis of aminocarbene complexes

### 2.3.1. General

**2.3.1.1. Chemicals for carbene complexes.** All experiments were carried out under argon. Tetrahydrofuran was distilled from benzophenone ketyl under argon prior to use. Chromium hexacarbonyl and  $\text{Me}_3\text{SiCl}$  were purchased from Aldrich and were used without purification. Silica and alumina were obtained from Merck. *N,N*-dimethylfuran-2-carboxamide, *N,N*-dimethylfuran-3-carboxamide were obtained by the reaction of the corresponding acylchloride with excess of *N,N*-dimethylamine in diethylether. *N,N*-dimethylthiophene-2-carboxamide [19], *N,N*-dimethylthiophene-3-carboxamide [19], 2-bromo-1-methylpyrrole[20], 3-bromo-1-methylpyrrole[20] were prepared according to the reported procedures. Melting points were determined on a Kofler block and are uncorrected.  $^1\text{H}$  and  $^{13}\text{C}$  NMR spectra were recorded on a Varian Gemini 300 spectrometer ( $^1\text{H}$  at 300 MHz,  $^{13}\text{C}$  at 75.4) in  $\text{CDCl}_3$ .

**2.3.1.2. General procedure for the preparation of chromium aminocarbene complexes.** The solution of sodium naphthalenide prepared from sodium (0.170 g, 7.4 mmol), naphthalene (0.947 g, 7.4 mmol) in THF (5 mL) was slowly added under argon atmosphere to the stirred suspension of  $\text{Cr}(\text{CO})_6$  (0.63 g, 2.9 mmol) in THF (10 mL) at  $-78^\circ\text{C}$ . The mixture was allowed to warm to  $0^\circ\text{C}$  and kept at this temperature until all solid carbonyl dissolved (0.5 h). After cooling to  $-78^\circ\text{C}$  a solution of the corresponding amide (2.0 mmol) in THF (5 mL) was added through a double-ended needle. The mixture was stirred at  $-78^\circ\text{C}$  for 30 min and then 30 min at  $0^\circ\text{C}$ . After cooling to  $-78^\circ\text{C}$ ,  $\text{Me}_3\text{SiCl}$  (0.73 mL; 5.7 mmol) was added via a syringe. The solution was stirred at  $-78^\circ\text{C}$  for 30 min, then the cooling bath was removed, the mixture was allowed to warm to  $0^\circ\text{C}$  and neutral alumina (8 g) was added. The solvent was removed under reduced pressure on a rotatory evaporator (bath temperature  $<30^\circ\text{C}$ ) and the residue was dried under high vacuum to remove all the THF. Then the sample was transferred on the top of a column filled with 50 g of silica. Naphthalene was eluted with pure hexane and further elution with a hexane- $\text{CH}_2\text{Cl}_2$  mixture gave the product

### 2.3.2. Pentacarbonyl[(*N,N*-dimethylamino)(2-furyl)carbene]chromium(0) (IIa)

Mixture of hexane-dichloromethane (2:1) was used for the elution. Yellow crystals, yield 41%, M.p.  $60\text{--}63^\circ\text{C}$ .  $^1\text{H}$  NMR (300 MHz,  $\text{CDCl}_3$ ):  $\delta$  3.32 (s, 3H,  $\text{CH}_3$ ), 3.97 (s, 3H,  $\text{CH}_3$ ), 6.33 (m, 1H, CH), 6.48 (m, 1H, CH), 7.50 (m, 1H, CH).  $^{13}\text{C}$  NMR (75 MHz,  $\text{CDCl}_3$ ):  $\delta$  48.1, 51.5, 107.8, 111.4, 142.3, 158.7, 217.0, 223.8, 260.5. IR: 3162, 3141, 2993, 2951, 2925, 2854, 2054, 1976, 1944, 1863, 1786, 1551, 1524, 1457, 1400, 1381, 1223, 1247, 1204, 1163, 1118, 1087, 1033, 1027,

946, 886, 848, 811, 755, 678  $\text{cm}^{-1}$ . Anal. Calcd for  $\text{C}_{12}\text{H}_9\text{CrNO}_6$ : C, 45.73; H, 2.88; N, 4.44. Found: C, 45.70; H, 3.27; N, 4.19.

### 2.3.3. Pentacarbonyl[(*N,N*-dimethylamino)(3-furyl)carbene]chromium(0) (IIb)

It was prepared in a different way according to the reported procedure [18].

### 2.3.4. Pentacarbonyl[(*N,N*-dimethylamino)(2-thienyl)carbene]chromium(0) (IIIa)

Mixture of hexane-dichloromethane (2:1) was used for the elution. Yellow crystals, yield 65%, M.p.  $>87^\circ\text{C}$  (decomp.).  $^1\text{H}$  NMR (300 MHz,  $\text{CDCl}_3$ ):  $\delta$  3.22 (s, 1H,  $\text{CH}_3$ ), 4.00 (s, 1H,  $\text{CH}_3$ ), 6.53 (m, 1H, CH), 6.98 (m, 1H, CH), 7.29 (m, 1H, CH).  $^{13}\text{C}$  NMR (75 MHz,  $\text{CDCl}_3$ ):  $\delta$  46.6, 51.4, 118.2, 123.9, 127.0, 152.9, 216.8, 223.7, 270.2. IR: 2056, 1973, 1937, 1879, 1810, 1794, 1542, 1511, 1435, 1401, 1234, 1160, 1103, 1077, 1041, 1019, 935, 851, 825, 793, 741, 693, 669,  $\text{cm}^{-1}$ . Anal. Calcd for  $\text{C}_{12}\text{H}_9\text{CrNO}_5\text{S}$ : C, 43.51; H, 2.74; N, 4.23. Found: C, 43.19; H, 2.99; N, 3.82.

### 2.3.5. Pentacarbonyl[(*N,N*-dimethylamino)(3-thienyl)carbene]chromium(0) (IIIb)

Mixture of hexane-dichloromethane (4:1) was used for the elution. Yellow crystals, yield 48%, M.p.  $70\text{--}73^\circ\text{C}$ .  $^1\text{H}$  NMR (300 MHz,  $\text{CDCl}_3$ ):  $\delta$  3.10 (s, 3H,  $\text{CH}_3$ ), 3.96 (s, 3H,  $\text{CH}_3$ ), 6.66 (m, 2H, CH), 7.37 (br s, 1H, CH).  $^{13}\text{C}$  NMR (75 MHz,  $\text{CDCl}_3$ ):  $\delta$  46.0, 51.0, 112.6, 121.8, 126.7, 153.3, 217.1, 223.7, 272.4. IR: 3742, 3121, 2951, 2871, 2053, 1975, 1939, 1917, 1848, 1544, 1514, 1451, 1401, 1357, 1233, 1211, 1176, 1118, 1083, 1025, 955, 870, 845, 785, 753, 695, 678, 663  $\text{cm}^{-1}$ . Anal. Calcd for  $\text{C}_{12}\text{H}_9\text{CrNO}_5\text{S}$ : C, 43.51; H, 2.74; N, 4.23. Found: C, 42.98; H, 2.92; N, 4.19.

### 2.3.6. Pentacarbonyl[(*N,N*-dimethylamino)(1-methyl-2-pyrrolyl)carbene]chromium(0) (IVa)

To the solution of 2-bromo-1-methylpyrrole (1.87 g, 11.7 mmol) in THF (60 mL) *n*-BuLi (7.30 mL, 11.7 mmol, 1.6 M solution in hexane) and TMEDA (1.70 mL, 11.7 mmol) in THF (60 mL) were added at  $-78^\circ\text{C}$ . The resulting mixture was stirred 30 min at  $-78^\circ\text{C}$  and then was allowed to warm to  $0^\circ\text{C}$ . To such prepared solution of 1-methyl-2-pyrrolyllithium chromium hexacarbonyl (3.08 g, 14.0 mmol) was added and the resultant mixture was stirred 12 h at room temperature. The solvents were then evaporated in vacuo at  $0^\circ\text{C}$ . The residue was dissolved in  $\text{CH}_2\text{Cl}_2$  (50 mL), cooled to  $-30^\circ\text{C}$  followed by dropwise addition of acetyl bromide (0.87 mL, 11.7 mmol). The mixture was then stirred 30 min at  $-10^\circ\text{C}$  and after recooling to  $-40^\circ\text{C}$  dimethylamine (20.0 mL, 20.0 mmol of 1 M solution in  $\text{Et}_2\text{O}$ ) was added. The mixture was stirred for 1 h without cooling, and neutral alumina (5 g) was added. Solvents were removed under reduced pressure, and the residue was dried under high vacuum. Column chromatography (silica gel, hexane-dichloromethane, 2:1) afforded the title carbene complex. Yellow crystals, yield 46%, M.p.  $>85^\circ\text{C}$  (decomp.).  $^1\text{H}$  NMR (300 MHz,  $\text{CDCl}_3$ ):  $\delta$  3.04 (s, 3H,  $\text{CH}_3$ ), 3.33 (s, 3H,  $\text{CH}_3$ ), 3.99 (s, 3H,  $\text{CH}_3$ ), 5.85 (m, 1H, CH), 6.15 (m, 1H, CH), 6.52 (m, 1H, CH).  $^{13}\text{C}$  NMR (75 MHz,  $\text{CDCl}_3$ ):  $\delta$  33.6, 46.1, 50.5, 102.7, 108.7, 120.4, 142.9, 216.8, 224.0, 272.8. IR: 2945, 2052, 1973, 1889, 1536, 1517, 1469, 1442, 1397, 1350, 1297, 1230, 1176, 1120, 1085, 1053, 1024, 1006, 900, 832, 776, 702, 660, 646, 604, 591, 559, 455  $\text{cm}^{-1}$ . Anal. Calcd for  $\text{C}_{13}\text{H}_{12}\text{CrN}_2\text{O}_5$ : C, 47.57; H, 3.68; N, 8.53. Found: C, 47.21; H, 3.65; N, 8.48.

### 2.3.7. Pentacarbonyl[(*N,N*-dimethylamino)(1-methyl-3-pyrrolyl)carbene]chromium(0) (**IVb**)

To the solution of 3-bromo-1-methylpyrrole (2.25 g, 14.0 mmol) in THF (60 mL) *n*-BuLi (8.80 mL, 14.0 mmol, 1.6 M solution in hexane) and TMEDA (2.01 mL, 14.0 mmol) in THF (60 mL) were added at  $-78^{\circ}\text{C}$ . The resulting mixture was stirred 30 min at  $-78^{\circ}\text{C}$  and then was allowed to warm to  $0^{\circ}\text{C}$ . To such prepared solution of 1-methyl-3-pyrrolyllithium chromium hexacarbonyl (3.30 g, 15.0 mmol) was added and the resultant mixture was stirred 12 h at room temperature. The solvents were then evaporated in vacuo at  $0^{\circ}\text{C}$ . The residue was dissolved in  $\text{CH}_2\text{Cl}_2$  (50 mL), cooled to  $-30^{\circ}\text{C}$  followed by dropwise addition of acetyl bromide (1.04 mL, 14.0 mmol). The mixture was then stirred 30 min at  $-10^{\circ}\text{C}$  and after recooling to  $-40^{\circ}\text{C}$  dimethylamine (35.0 mL, 35.0 mmol, 1 M solution in  $\text{Et}_2\text{O}$ ) was added. The mixture was stirred for 1 h without cooling, and neutral alumina (5 g) was added. Solvents were removed under reduced pressure, and the residue was dried under high vacuum. Column chromatography (silica gel, hexane–dichloromethane, 1:2) afforded the title carbene complex in the form of yellow oil, yield 51%.  $^1\text{H NMR}$  (300 MHz,  $\text{CDCl}_3$ ):  $\delta$  3.26 (s, 3H,  $\text{CH}_3$ ), 3.64 (s, 3H,  $\text{CH}_3$ ), 3.91 (s, 3H,  $\text{CH}_3$ ), 5.75 (m, 1H, CH), 6.39 (t,  $J = 1.8$  Hz, 1H, CH), 6.54 (t,  $J = 2.4$  Hz, 1H, CH).  $^{13}\text{C NMR}$  (75 MHz,  $\text{CDCl}_3$ ):  $\delta$  36.1, 46.0, 51.2, 103.5, 115.2, 121.7, 138.3, 217.8, 224.3, 269.4. IR: 2944, 2049, 1969, 1867, 1519, 1448, 1419, 1399, 1331, 1214, 1179, 1122, 1084, 1026, 1002, 985, 940, 815, 769, 705, 658, 642, 594, 562,  $456\text{ cm}^{-1}$ . Anal. Calcd for  $\text{C}_{13}\text{H}_{12}\text{CrN}_2\text{O}_5$ : C, 47.57; H, 3.68; N, 8.53. Found: C, 47.13; H, 3.83; 8.45.

The compound **I** was prepared as described elsewhere [18].

## 3. Results and discussion

The following discussion is based on comparison of the compounds **IIa**, **IIb**, **IIIa**, **IIIb**, **IVa** and **IVb** with the reference compound **I**.

### 3.1. Electrochemical oxidation

The oxidation reaction was followed on a GC-disk electrode, either rotating (voltammetry, controlled-potential electrolyses) or stationary (cyclic voltammetry) in nonaqueous acetonitrile. In case of **I**, a one-electron process occurs and the curve exhibited partial reversibility at room temperature. During preparative oxidation small bubbles were observed at the surface of the electrode. The primary electrochemical oxidation is most probably followed by a relatively slow decomposition of the molecule **I** accompanied by release of CO gas. This interpretation was confirmed by IR spectroelectrochemistry: in the course of oxidation of **I**, the bands belonging to CO groups vibrations (at  $1930\text{ cm}^{-1}$ ) disappeared (Fig. 2a).

When the phenyl group is replaced by a five-membered heterocycle (**IIa**, **IIb**, **IIIa**, **IIIb**, **IVa**), the oxidation pattern is similar, however, the reversibility is partially lost and the one-electron quasi-reversible oxidation process was clearly observed after cooling to  $0^{\circ}\text{C}$  (as evident from the peak difference,  $\Delta E$  and the  $i_c/i_a$  ratio – Table 1, Fig. 3). The presence of the cathodic counterpeak enables to estimate  $E_{\text{ox}}$  values. With increasing temperature the reversibility decreases so that no reversal peak appeared at room temperature (except **IIa**, where the reversibility is preserved). The analogy of the follow-up reaction with **I** is evident from IR spectroelectrochemical results during preparative electrolysis of **IIa** where disappearance of CO groups was also observed (Fig. 2b). Thus, in comparison to **I**, the oxidation of **II–IV** exhibits lower reversibility caused probably by faster decomposition reaction.

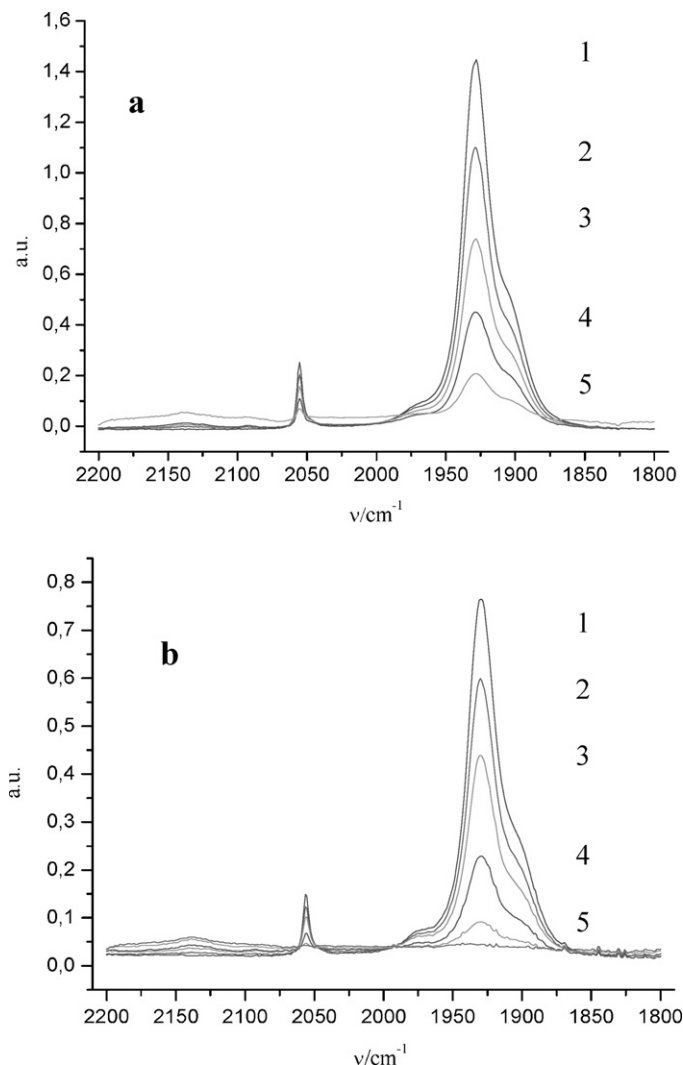


**Fig. 2.** Oxidative electrolysis of (a) **I** and (b) **IIa**, followed by IR spectra. Time of electrolysis: curve 1: 0 min (before electrolysis); curve 2: 3 min; curve 3: 6 min; curve 4: 9 min; curve 5: 12 min.

The difference in oxidation potentials between **IIa** and **IIb** (and similarly between **IIIa** and **IIIb**, i.e. between the derivatives with the heterocycle bound in positions 2- and 3-, respectively) is very small. This means that the mesomeric effect and eventual change in delocalization of  $\pi$  electrons in the carbene ligand moiety plays no significant role toward oxidation potential.

On the other hand, the inductive influence of the heterocycle itself (i.e. of the heteroatom) is evident: the oxidation potentials (cf. Table 1) decrease linearly in the sequence **II** (furyl) > **III** (thienyl) > **IV** (*N*-methylpyrrolyl), according to the LFER model when used, sigma aryl values ( $\sigma_a$ ) [21]. This corresponds to the increasing electron donor ability, which is in the case of **IV** even enhanced by the presence of the methyl substituent.

All oxidation potentials of **IIa**, **IIb**, **IIIa**, **IIIb**, **IVa** appeared between 0.83 and 0.90 V vs. SCE, in the same potential region as the  $E_{\text{ox}}$  values acquired for **I** and its derivatives [(CO) $_5$ Cr = C(NR $_2$ )(*p*-R-Ph)] [8]. This fact points to the comparable (and small) inductive influence of phenyl ring and five membered heterocycles (except **IVb**) on the course of the oxidation of studied compounds. The electron transfer takes place on the metal center, initiating a slow decomposition of the carbonyl complex. No electrochemical polymerization of the heterocyclic substituents was observed.

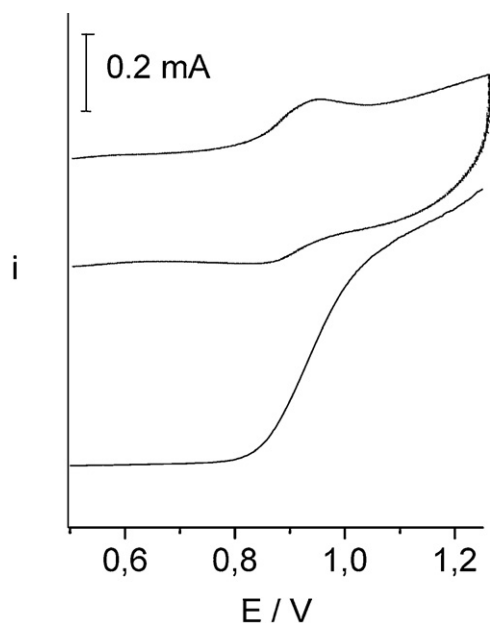


Fig. 3. Cyclic voltammogram at 0°C and rotating disk voltammogram at glassy carbon electrode of the oxidation of the compound **IIIa**.

The behavior of **IVb** is slightly different. The signs of reversibility were not observed even under cooling and at higher scan rate, its oxidation is the easiest from the whole series. Whereas in all other compounds the oxidation peak potential decreases after cooling, in the case of **IVb**  $E_{pa}$  at 0°C is more positive than at the laboratory temperature. The reason for the difference is not yet clear.

### 3.2. Electrochemical reduction

Electrochemical reduction was studied by polarography and by cyclic voltammetry on HMDE and GC. For the exhaustive electrolyses a mercury-pool electrode was used. Reduction of all studied molecules proceeds irreversibly, reduction potential was determined as a polarographic half-wave potential ( $E_{1/2}$ ). CV measurements were used to compare the respective oxidation and reduction peak currents and influence of the electrode material on the overall process. As a result, the reduction currents correspond to two-electron processes, the difference between the electrode

Table 1  
Cyclic voltammetry data (GC, AN/TBAPF<sub>6</sub>, SCE, scan rate 100 mV s<sup>-1</sup>).

Compound	$\sigma_a$	$t/^\circ\text{C}$	$E_{pa}$ vs SCE/V	$\Delta E/\text{V}$	$E_{ox}$ vs SCE/V	$i_c/i_a$
<b>I</b>		25	0.862	0.072	0.826	0.692
<b>IIa</b>	1.08	25	0.959	0.121	0.899	0.430
		0	0.940	0.087	0.897	0.860
<b>IIIa</b>	0.71	25	0.944	–	–	–
		0	0.914	0.106	0.856	0.280
<b>IVa</b>	–0.40	25	0.894	–	–	–
		0	0.858	0.065	0.826	0.493
<b>IIb</b>	0.25	25	0.954	–	–	–
		0	0.924	0.101	0.874	0.389
<b>IIIb</b>	0.12	25	0.954	–	–	–
		0	0.872	0.080	0.832	0.792
<b>IVb</b>	–1.08	25	0.792	–	–	–
		0	0.823	–	–	–

$\sigma_a$  – sigma “aryl” values [21].

$\Delta E = E_{pa} - E_{pc}$ .

$E_{ox} = \frac{1}{2}(E_{pa} + E_{pc})$ .

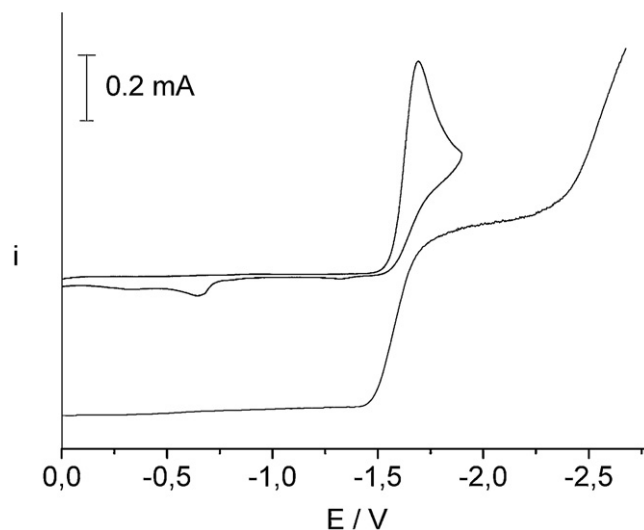


Fig. 4. Cyclic voltammogram at HMDE and the polarographic curve of the reduction of the compound **IIIa**.

materials is minimal, nevertheless, mercury offers better curves and wider potential window (Fig. 4).

The results are summarized in Table 2. (For comparison, under given conditions,  $E_{1/2}$  value for the compound **I** is –1.995 V vs. SCE.). When comparing the O-, S- and N-heterocycles, the behavior of furyl and thienyl derivatives is analogous, i.e. the data as well as their relationship are similar. On the other hand, the electrochemical properties of N-methylpyrrol derivatives are partly different. Therefore, the results concerning compounds **IIa,b** and **IIIa,b** will be discussed separately from the molecules **IVa,b** bearing 1-methylpyrrolyl group.

The compounds **IIa,b** and **IIIa,b** are in all cases reduced more easily than **I** ( $E_{red}(\text{I}) = -1.995$  V). Whereas the reduction potentials of the molecules bearing the heterocycle bound in position 3 (**IIb** and **IIIb**) are only by 80–90 mV less negative than the phenyl derivative **I**, the compounds bearing the heterocycle bound in position 2 (**IIa** and **IIIa**) are reduced significantly more positively. The exchange of oxygen by sulphur has only negligible influence (about 10 mV) on the reduction potentials and the direction of the potential shift corresponds to the electronegativity difference between the two heteroatoms.

From the previous studies [7] it is known that the reduction center of the whole molecule is located on the carbene ligand and that it is influenced primarily by its substituents, in this case by the heterocycles. From Table 2, it is evident that the reduction potential is much more sensitive to the heterocycles attached by the position 2 (derivatives “a”) than by the position 3 (derivatives “b”). This substantial feature is given by different relative importance of inductive and mesomeric effects of the substituents:

The heterocycle attached by its position 3 cannot be involved in full conjugation with the carbene double bond, the  $\pi$ -delocalization is low and therefore the influence of the heterocycle is limited only to the inductive effect. On the other hand, the heterocycle attached by its position 2 allows formation of an enlarged  $\pi$ -system which makes the reduction much easier by stabilizing the reduction

Table 2  
 $E_{1/2}$  of the studied compounds. Values vs SCE/V.

Heterocycle	Binding site 2		Binding site 3	
Furan	–1.591	<b>IIa</b>	–1.909	<b>IIb</b>
Thiophene	–1.601	<b>IIIa</b>	–1.915	<b>IIIb</b>
1-Methylpyrrol	–1.894	<b>IVa</b>	–2.036	<b>IVb</b>

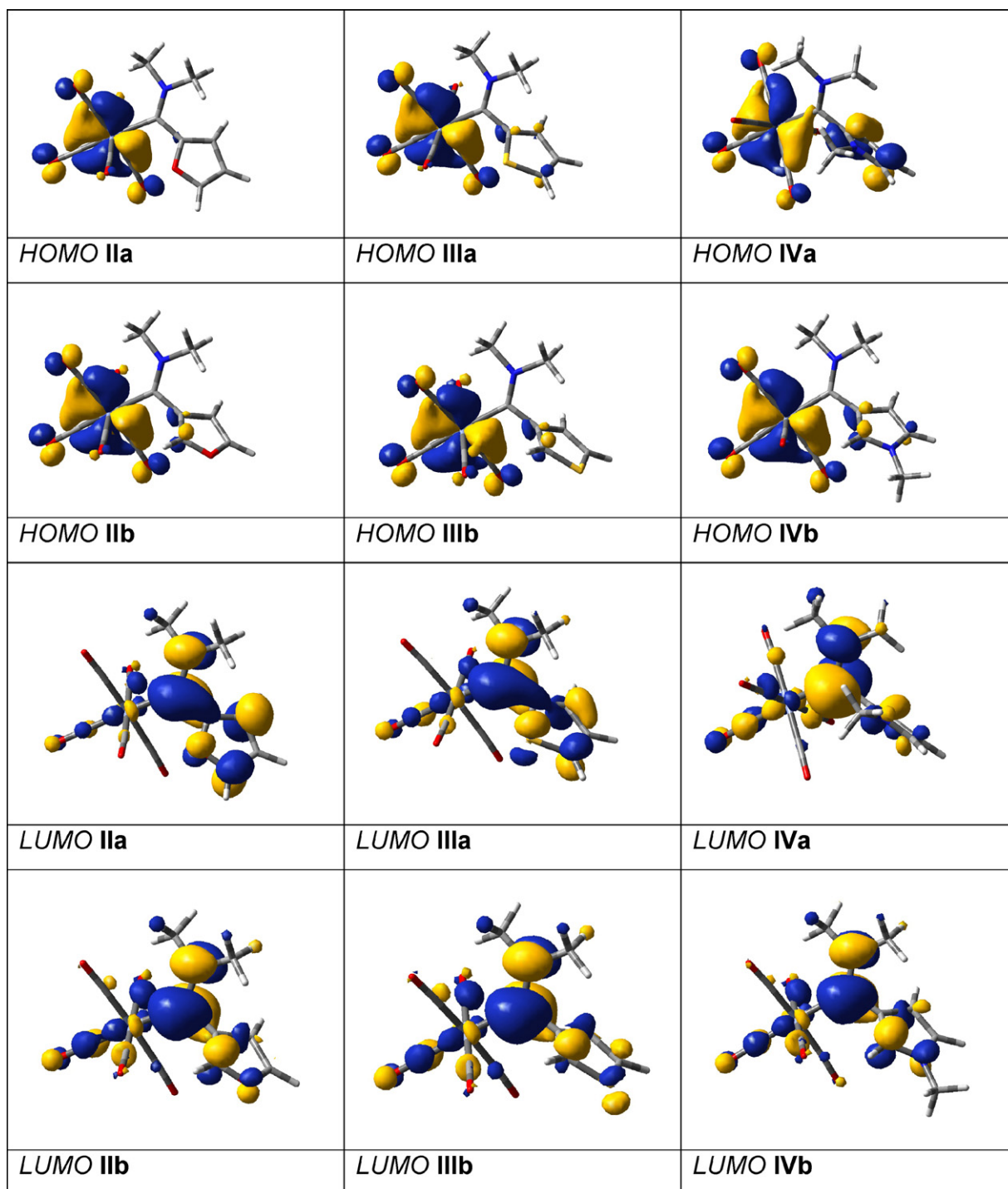


Fig. 5. Visualization of FMOs.

intermediate. Here the inductive effect of the substituent is completed by an even stronger mesomeric effect caused by the extension of electron delocalization to the heterocycle. Analogous effect was observed recently in the case of aminocarbenes of the type **I**, where the phenyl ring was substituted in *para*-position by a carbonyl [11].

Another argument supporting this conclusion is based on the well known ability of thiophene and pyrrole to form conducting polymers (i.e. large  $\pi$ -delocalized system) where the heterocycles are interconnected through the positions 2 and 5, but not 3.

The products of preparative electrolyses were separated using extraction of organic species from the electrolyzed solution to hexane. The MS spectra proved presence of *N,N*-dimethyl(thiophen-2-yl)methanamine. Hence the electrochemical reduction leads first to the splitting of the carbene bond C=Cr, the intermediate is then hydrogenated by traces of protons from the solvent. In a parallel electrolysis the IR spectra were simultaneously followed. The vibration bands of CO groups are present even after exhaustive electrolysis but their number and energy was changed. This means that in the split-off metal part, the Cr–CO bonds retained, but the

**Table 3**  
Contributions (%) of individual molecular fragments to FMOs.

		Cr(CO) <sub>5</sub>	C <sub>carb</sub>	NMe <sub>2</sub>	Heterocycle
<b>IIa</b>	HOMO	96	3	0	2
	LUMO	11	35	17	37
<b>IIb</b>	HOMO	93	2	0	4
	LUMO	17	47	21	15
<b>IIIa</b>	HOMO	92	2	0	6
	LUMO	13	41	20	27
<b>IIIb</b>	HOMO	92	2	0	5
	LUMO	17	47	21	15
<b>IVa</b>	HOMO	75	2	0	22
	LUMO	16	50	22	13
<b>IVb</b>	HOMO	90	2	0	7
	LUMO	17	45	20	19

resulting carbonyl complexes are rearranged and have different (and lower) symmetry.

### 3.3. Quantum chemical calculations

The above-mentioned interpretation of experimental electrochemical data was correlated with quantum chemical calculations of frontier molecular orbitals (FMOs) of studied molecules focusing on the electron delocalization. The HOMOs are very similar for all studied heterocyclic derivatives being always localized on the chromium atom and CO ligands. On the other hand, there is a clear difference between the LUMOs of “a” and “b” derivatives. (Visualizations of the orbitals are shown in Fig. 5 and their composition is summarized in Table 3). The heterocycle attached in the position 2 forms with the carbene grouping an extended delocalized system involving substantially also the heterocycle, resulting in easier reducibility of the 2-het derivatives in contrast to the 3-het ones. Percentual composition of LUMOs confirms that the orbitals of the heterocycle are much more involved in 2-het derivatives whereas in the 3-het derivatives, the LUMOs are located prevalently on the carbene carbon and the amino group.

To get further support for the above-mentioned interpretation, structures of complexes after one-electron oxidation or reduction were optimized. The electronic structure changes from uncharged diamagnetic to charged paramagnetic configuration under relaxation of the whole molecule. To show the localization of this unpaired electron, free spin density was examined in the relaxed oxidized and reduced species, respectively. The spin density distribution for 2-thienyl derivative (**IIIa**) is depicted at Fig. 6, the results for the other derivatives are analogous.

In case of the oxidized molecules the unpaired electron is localized prevalently on the metal center, hence the oxidation takes place in this part of the complex. On the other hand, in the reduced species the spin density is found mainly on the carbene ligand and is delocalized across the heterocycle residue. This confirms that the reduction takes place on the carbene ligand and illustrates the importance of electronic conjugation throughout this ligand.

### 3.4. 1-Methylpyrrolyl derivatives

The behavior of molecules substituted by 1-methylpyrrolyl group, **IVa** and **IVb**, is somewhat different from that of furan and thiophene derivatives. First, the difference between the reduction potentials of **IVa** and **IVb** does not exceed 150 mV which is only half of the difference found for the compounds **II** and **III**. The reason is a sterical influence of the “ortho”-methyl group in the case of **IVa** and thus more difficult rotation of the pyrrol ring, preventing planarity and  $\pi$ -delocalization of the system carbene-heterocycle.

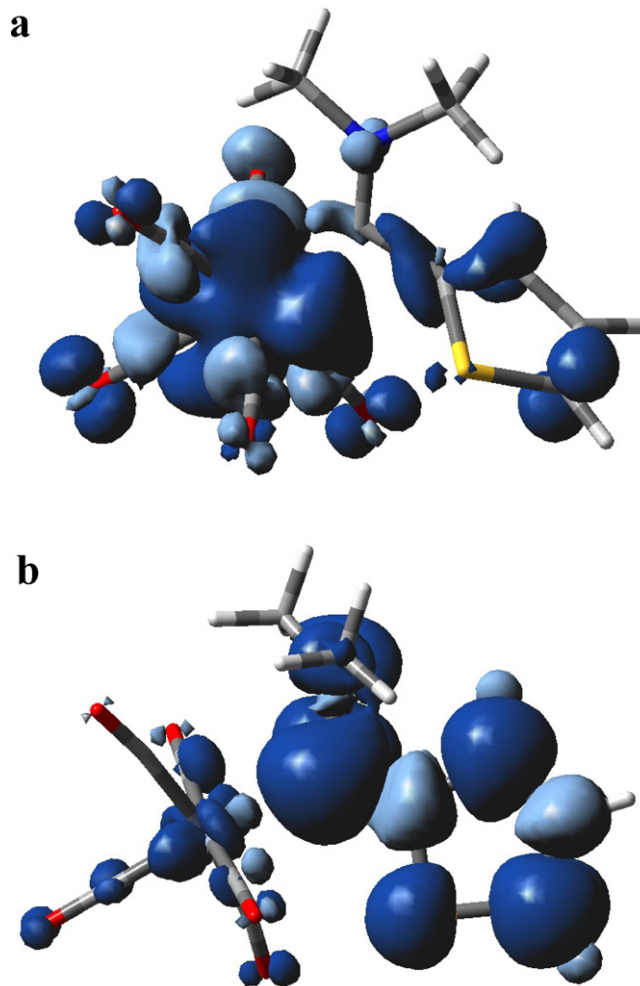


**Fig. 6.** Visualization of spin density distribution for oxidized (a) and reduced (b) 2-thienyl derivative (**IIIa**).

This is why the reduction potential of the compound **IVa** is shifted to the less negative potentials only slightly. We have shown recently a similar case [8] that the hindered rotation of *ortho*-substituted phenyl ring causes more difficult reduction.

The above-mentioned relatively negative reduction potential of **IVa** and the fact that  $E_{\text{red}}$  of **IVb** is even more negative than  $E_{\text{red}}$  of **I** is evidently caused by presence of the methyl group, which due to its additive electron pushing effect shifts the reduction potentials to more negative values.

A substantial difference was observed also in the percentual distribution of HOMO orbitals: whereas the shape of HOMO of **IVb** fits well to the other compounds, as much as 22% of HOMO in the case of **IVa** is surprisingly located at the heterocycle. This effect is not yet understood and is subject of next investigations, simultaneously with the mentioned anomalies in the oxidation potentials.

## 4. Conclusions

A new series of aminocarbene complexes of chromium(0) was synthesized, where the carbene ligand bears various five-membered heteroaromatic rings: furan, thiophene and N-Methylpyrrol, attached either by their position 2 or 3. The compounds were characterized by <sup>1</sup>H and <sup>13</sup>C NMR and elemental analysis. The aim of the electrochemical investigation was to understand the role of the heterocyclic substituent in the structure-properties relationship.

Using cyclic voltammetry and IR-spectroelectrochemistry it was found that the originally reversible one-electron oxidation localized on the metal center of the complexes is followed by a slow decarbonylation. Nevertheless, neither different heterocycle, nor different position of its attachment can significantly influence the oxidation behavior, including the oxidation potential itself. This observation points to a very limited electronic communication between the metal center and the carbene ligand.

In the case of reduction of the title compounds, which is two-electron, irreversible, the potentials are affected both by the heterocycle and by the position of its attachment. The nature of the heteroatom has rather inductive effect, according to expectations. On the other hand, the position by which the heterocycle is bound to the carbene carbon decides about extension of the  $\pi$ -electron delocalization along the carbene ligand and the mesomeric effect plays the significant role. As a result, the heterocycle attached by its position 2 is much more involved in the LUMO orbital than the heterocycle attached by its position 3, causing the reduction potential shift by about 300 mV to lower values. This relative contribution of inductive and mesomeric effects of the heterocycles to the reduction of the chromium aminocarbenes was discussed in comparison with the previously studied phenyl substituted derivatives.

The situation in N-methylpyrroles is complicated by the steric influence of the methyl substituent and thus by the hindered rotation of the heterocycle preventing partly the overlap of orbitals.

The interpretation was confirmed by quantum chemical calculations of the shape of HOMO–LUMO orbitals and of the percentual contribution of individual molecular fragments to the FMOs.

The IR and MS identification of products of preparative electrolyses allowed discussing the probable mechanisms: Whereas at positive potentials the originally reversible oxidation of the low-valent chromium is followed by slow decomposition of the complex accompanied by decarbonylation, during reduction the carbene C=Cr bond is split under formation of reduced ligand (N,N-dimethyl(thiophen-2-yl)methanamine), the split-off metal part is then rearranged (formation of bi- or polynuclear complexes cannot be excluded), but the form of carbonyl complex is preserved.

## Acknowledgements

The authors are grateful to Dr. Stanislav Záliš (J. Heyrovský Institute) for valuable discussions and comments. Financial support was provided by the GA AV CR (grant No. IAA 00400813).

## References

- [1] L.S. Hegedus, *Transition Metals in the Synthesis of Complex Organic Molecules*, University Science Books, 1994.
- [2] K.H. Dotz, J. Stendel, *Journal of Chemical Reviews* 109 (2009) 3227.
- [3] J. Santamaría, *Journal of Current Organic Chemistry* 13 (2009) 31.
- [4] S. Watanuki, N. Ochifuji, M. Mori, *Organometallics* 14 (1995) 4129.
- [5] M.A. Fernández-Rodríguez, P. García-García, E. Aguilar, *Chemical Communications* 64 (2010) 7670.
- [6] P. Zuman, *Substituent Effects in Organic Polarography*, Plenum Press, New York, 1967.
- [7] I. Hoskovcová, J. Roháčová, L. Meca, T. Tobrman, D. Dvořák, J. Ludvík, *Electrochimica Acta* 50 (2005) 4911.
- [8] I. Hoskovcová, J. Roháčová, D. Dvořák, T. Tobrman, S. Záliš, R. Zvěřinová, J. Ludvík, *Electrochimica Acta* 55 (2010) 8341.
- [9] W. Kaim, B. Schwederski, *Coordination Chemistry Reviews* 254 (2010) 1580.
- [10] A.B.P. Lever, *Coordination Chemistry Reviews* 254 (2010) 1397.
- [11] I. Hoskovcová, R. Zvěřinová, J. Roháčová, D. Dvořák, T. Tobrman, S. Záliš, J. Ludvík, *Electrochimica Acta* 56 (2011) 6853.
- [12] M. Krejčík, M. Daněk, F. Hartl, *Journal of Electroanalytical and Chemical Interfacial Electrochemistry* 317 (1991) 179.
- [13] M.J. Frisch, G.W. Trucks, H.B. Schlegel, G.E. Scuseria, M.A. Robb, J.R. Cheeseman, G. Scalmani, V. Barone, B. Mennucci, G.A. Petersson, H. Nakatsuji, M. Caricato, X. Li, H.P. Hratchian, A.F. Izmaylov, J. Bloino, G. Zheng, J.L. Sonnenberg, M. Hada, M. Ehara, K. Toyota, R. Fukuda, J. Hasegawa, M. Ishida, T. Nakajima, Y. Honda, O. Kitao, H. Nakai, T. Vreven, J.A. Montgomery Jr., J.E. Peralta, F. Ogliaro, M. Bearpark, J.J. Heyd, E. Brothers, K.N. Kudin, V.N. Staroverov, T. Keith, R. Kobayashi, J. Normand, K. Raghavachari, A. Rendell, J.C. Burant, S.S. Iyengar, J. Tomasi, M. Cossi, N. Rega, J.M. Millam, M. Klene, J.E. Knox, J.B. Cross, V. Bakken, C. Adamo, J. Jaramillo, R. Gomperts, R.E. Stratmann, O. Yazyev, A.J. Austin, R. Cammi, C. Pomelli, J.W. Ochterski, R.L. Martin, K. Morokuma, V.G. Zakrzewski, G.A. Voth, P. Salvador, J.J. Dannenberg, S. Dapprich, A.D. Daniels, O. Farkas, J.B. Foresman, J.V. Ortiz, J. Cioslowski, D.J. Fox, Gaussian 097, Revision B.01, Gaussian Inc., Wallingford, CT, 2010.
- [14] A.D. Becke, *Journal of Chemical Physics* 98 (1993) 5648.
- [15] A.D. Becke, *Phys. Rev. A* 38 (1988) 3098.
- [16] P.C. Hariharan, J.A. Pople, *Theor. Chim. Acta* 28 (1973) 213.
- [17] V.A. Rassolov, J.A. Pople, M.A. Ratner, T.L. Windus, *Journal of Chemical Physics* 109 (1998) 1223.
- [18] R. Imwinkelried, L.S. Hegedus, *Organometallics* 7 (1988) 702.
- [19] M. Davis, R. Lakhani, B. Ternai, *Journal of Organic Chemistry* 41 (1976) 3591.
- [20] E. Dvornikova, K. Kamińska-Trela, *Synlett* (2002) 1152.
- [21] O. Exner, A critical compilation of substituent constants, in: N.B. Chapman, J. Shorter (Eds.), *Correlation Analysis in Chemistry*, Plenum Press, N.Y., London, 1978, pp. 445.